JOURNAL OF SOLID STATE CHEMISTRY 60, 51–61 (1985)

Chemical Composition and Crystal Structure of β-Alumina Type R^+-Gallate ($R^+ = K^+, NH_4^+$)

H. IKAWA, T. TSURUMI, M. ISHIMORI, K. URABE, AND S. UDAGAWA

Department of Inorganic Materials, Faculty of Engineering, Tokyo Institute of Technology, 12-1, Ookayama 2-chome, Meguro-ku, Tokyo 152, Japan

Received October 26, 1984; in revised form April 8, 1985

The crystal structures of β-alumina type K^+-gallate (K^+-β-gallate), Mg^{2+}-doped K^+-β-gallate, and NH_4^+-β-gallate were refined by the single crystal X-ray diffraction method. The positive charges of excess K^+ ions in K^+-β-gallate were compensated by O^{2-} ions in the *mO* site which coordinated with interstitial Ga^{3+} ions. The charge compensation mechanism mentioned above was changed by doping with Mg^{2+} ions. The excess charges in Mg^{2+}-doped K^+-β-gallate were compensated by the replacement of Mg^{2+} ions for Ga^{3+} ions at the middle of spinel block. No defects were found in NH_4^+-β-gallate for the charge compensation, which was completely consistent with the result of thermal analysis that indicated a stoichiometric composition of NH_4^+-β-gallate.

Introduction

It is well known that β-alumina (ideal formula $Na_2O \cdot 11Al_2O_3$) exhibits a high sodium ion conduction and is one of the most widely studied solid electrolytes. There are many studies on the crystal structures of the β-alumina type compounds, in which the distribution of the alkali ions in the conduction plane and charge compensation mechanisms of the excess alkali ions have been studied by the X-ray (*1–8*) or neutron diffraction method (*9–11*).

It is also known that gallates with the β-alumina type structure (hereafter abbreviated as R^+-β-gallate after Chandrashekhar and Foster (*12*)) show high ionic conduction. The ionic conductivities of K^+-β-gallate and its solid solutions in which the contents of K^+ ions were controlled by doping with Mg^{2+} ions have been reported by Tsurumi *et al.* (*13*). It has been revealed that the amount of K^+ ions is less than that expected by a simple substitution model. The thermal decomposition of NH_4^+-β-gallate has been studied by Ikawa *et al.* (*14*) and their results indicated that the gallate contained a stoichiometric amount of NH_4^+ ions. Therefore, it seems to suggest that K^+-β-gallate, Mg^{2+}-doped K^+-β-gallate, and NH_4^+-β-gallate differed from one another with respect to the charge compensation mechanism of the excess positive charges. Although this suggest the need for extensive studies on the crystal structure of R^+-β-gallate, such studies are very few. Two of the studies reported so far are those of Anderson *et al.* (*15*) and Kahn *et al.* (*16*).

In the present study, an attempt has been made to refine the crystal structures of K^+-β-gallate, Mg^{2+}-doped K^+-β-gallate, and NH_4^+-β-gallate by the single crystal X-ray diffraction method. The results indicated that the charge compensation mechanism

0022-4596/85 $3.00

changed by doping with Mg^{2+} ions and that the defects which enable the excess alkali ions to exist are not found in NH_4^+-β-gallate.

Experimental

Experimental procedures for the preparation of single crystals and chemical analyses have been reported in the previous study (*13*). In the following, the experimental procedure is given briefly.

The reagents of Ga_2O_3, K_2CO_3, and $Mg(OH)_2$ were weighed in the molar ratio $5:1:X$ ($X = 0.0, 0.4$) and mixed with ethanol. After calcining at 900°C, the mixture was enclosed in a Pt · Rh-10% pipe with 10-mm diameter and 40-mm length. The sealed capsule was heated at 1800°C for 1 h and cooled gradually in a furnace. Single crystals of K^+-β-gallate were converted into NH_4^+-β-gallate by immersion in molten NH_4NO_3 for a duration up to 400 h. Chemical compositions of single crystals synthesized were analyzed by dissolving them into HCl solution, the contents of gallium and magnesium were determined by the atomic absorption analysis, and that of potassium was found by the flame spectrochemical analysis.

Refinements of the crystal structure were carried out for K^+-β-gallate, Mg^{2+}-doped K^+-β-gallate ($X = 0.4$), and NH_4^+-β-gallate. The space group of these crystals was identified as $P6_3/mmc$ from the systematic extinctions ($h\ k\ l$, $l = 2n + 1$) seen on Weissenberg photographs which is consistent with those space groups reported previously. X-Ray intensity data were collected with a four-circle diffractometer (Philips Co., PW1100) using Mo$K\alpha$ radiation with a graphite monochromator. The θ–2θ scanning was used for intensity data collections up to $2\theta = 100$ in a section of the reciprocal space where all $h > 0$, $k > 0$, and $l > 0$. There standard reflections were measured at intervals of 2h to monitor the drifts of the intensity and geometrical setting parameters. For weak intensity reflections, measurements were repeated 3 times until the total intensity counts exceeded 10,000. The structure factor (Fo) was calculated for each reflection, and then, anisotropic absorption corrections were performed with the program FDINCOR (*17*). Equivalent reflections were finally averaged and each parameter was refined with the full matrix program LINUS (*18*). Table I shows pertinent information such as the chemical compositions, sizes, and numbers of independent reflections. Chemical formulas are shown in the parenthesis. The formula for the Mg^{2+}-doped gallate was calculated by assuming that Mg^{2+} ions were substituted for Ga^{3+} ions in the spinel blocks.

Calculations for structural refinements

TABLE I

SOME DATA OF CRYSTAL STRUCTURE REFINEMENTS

	K^+-β-gallate	Mg^{2+}-doped K^+-β-gallate	NH_4^+-β-gallate
Chemical composition	$1.28K_2O \cdot 11Ga_2O_3$ ($K_{2.56}Ga_{22}O_{34.28}$)	$1.53K_2O \cdot 11Ga_2O_3 \cdot 0.92MgO$ ($K_{2.94}Ga_{21.12}Mg_{0.88}O_{34.03}$)	$(NH_4)_2O \cdot 11Ga_2O_3$ ($(NH_4)_2Ga_{22}O_{34}$)
Size of crystal (mm)	0.10 × 0.18 × 0.04	0.10 × 0.08 × 0.04	0.12 × 0.19 × 0.07
Lattice constants (Å)	a = 5.839(2)	5.857(1)	5.837(2)
	c = 23.47(1)	23.33(2)	23.59(1)
Number of independent reflections	949	556	998
Number of parameters	50	49	37

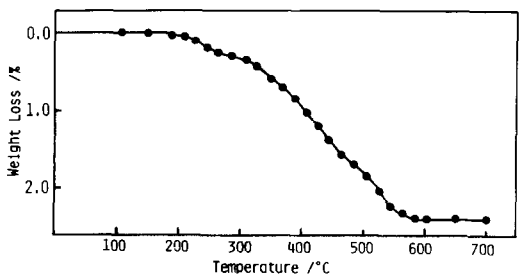

FIG. 1. The thermogravimetric curve of NH_4^+-β-gallate crystals obtained by changing the temperature step by step at 20–30°C intervals and keeping it constant at each temperature for 3 h.

were performed using the HITAC M-280 computer system.[1]

Results and Discussion

1. Chemical Compositions of Single Crystals

The chemical compositions for K^+-β-gallates with and without Mg doping are shown in Table I. The chemical formula for the Mg^{2+}-doped gallate indicates that 0.88 of Mg^{2+} ions per unit cell are substituted for Ga^{3+} ions in the crystal. If the increase in K^+ ions comes from the simple substitution, the formula should be $K_{3.44}Ga_{21.12}Mg_{0.88}O_{34.28}$. However, as indicated in the table, the content of K^+ ions determined by the chemical analysis (2.94) is less than expected (3.44). It was reported by Tsurumi *et al.* (*13*) that the contents of K^+ ions were consistently less than those estimated from the simple substitution.

[1] See NAPS document No. 04307 for 18 pages of supplementary material. Order form ASIS/NAPS, Microfiche Publications, P.O. Box 3513, Grand Central Station, New York, NY 10163. Remit in advance $4.00 for microfiche copy or for photocopy, $7.75 up to 20 pages plus $.30 for each additional page. All orders must be prepaid. Institutions and organizations may order by purchase order. However, there is a billing and handling charge for this service of $15. Foreign orders add $4.50 for postage and handling, for the first 20 pages, and $1.00 for additional 10 pages of material. Remit $1.50 for postage of any microfiche orders.

A thermogravimetric curve of single crystals of NH_4^+-β-gallate is shown in Fig. 1, which was measured on a differential type TG-DTA(Rigaku Denki Co.) by changing the temperature step by step at 20 to 30°C intervals and keeping it constant at each temperature for 3 h. Ikawa *et al.* (*14*) reported that the thermal decomposition of powder NH_4^+-β-gallate occurred as follows:

$$1.25H_2O \cdot (NH_4)_2O \cdot 11Ga_2O_3 \xrightarrow{\sim 180°C}$$

$$(NH_4)_2O \cdot 11Ga_2O_3 + 1.25H_2O \xrightarrow{\sim 230°C}$$

$$H_2O \cdot 11Ga_2O_3 + 2NH_3 \xrightarrow{> 460°C}$$

$$11Ga_2O_3 + H_2O$$

NH_4^+-β-gallate contains just a stoichiometric amount of NH_4^+ ions. The reaction formulas presented above show that some water is lost when heated up to 180°C, but the weight losses are not seen in Fig. 1, which indicated that electrically neutral water does not exist in the larger crystals (~0.5 mm). Foster *et al.* (*19*) have also reported that the amount of water in Na^+-β''-gallate varied with the size of the crystal. Since the liberation of NH_3 and H_2O at high temperatures does not seem to attain equilibrium within 3 h, weight losses due to the release of H_2O and NH_3 are overlapping each other in Fig. 1 and it is difficult to evaluate the amount of NH_3 and H_2O released separately. However, the total weight loss observed (2.4%) is consistent with that calculated (2.46%) assuming that two moles of NH_3 and one mole of H_2O are released per 11 Ga_2O_3. The chemical composition of the NH_4^+-β-gallate crystals is, therefore, $(NH_4)_2O \cdot 11Ga_2O_3$ (Table I).

2. Refinements of the Crystal Structure

(*a*) *K^+-β-Gallate*

Starting positional parameters used for the refinements were those of Peters *et al.* (*2*). With an occupancy factor of K^+ ion in the *BR* site fixed at the ideal value, the posi-

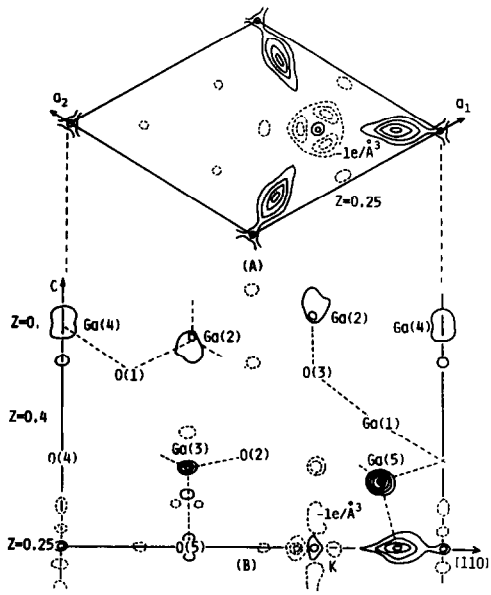

FIG. 2. Difference Fourier maps of K^+-β-gallate when R factor is 0.0677. (A) conduction plane at Z = 0.25; (B) (110) plane. Solid contours are drawn at intervals of $1e/Å^3$, and dashed contours at intervals of $1e/Å^3$.

tional parameters and anisotropic temperature factors were refined for all atoms (R = 0.0677).[2] Figure 2 shows difference Fourier maps in the conduction plane at Z = 0.25 (A) and in (110) plane (B) at this stage. A valley of electron density distribution is seen at the *BR* site, while positive peaks are seen at the *m*O sites in the conduction plane (A). In the (110) plane (B), a notable positive peak is seen at the Ga(5) site which is tetrahedrally coordinated by O(4), two O(2), and O^{2-} ion in the *m*O sites. Subsequently, we refined the occupancy factors of K^+ ion in the *BR* and *m*O sites (R = 0.0584), and those of the Ga(1) and Ga(5) sites under the restriction that the occupancy of O atom in the *m*O site was half that of the Ga atom in the Ga(5) site (R = 0.044). Finally, the occupancy of K^+ ion in the *aBR* site and the parameters of other atoms were refined again (R = 0.0388). The final parameters such as the numbers of atoms per unit cell, the positional parameters and anisotropic temperature factors are listed in Table IIA.

[2] The value of the reliability factor (R factor) at each stage of the refinement is noted in parentheses in the following descriptions.

(*b*) *Mg^{2+}-Doped K^+-β-Gallate*

Starting positional parameters were those of the K^+-β-gallate crystal determined by the foregoing refinements. The positional parameters and anisotropic temperature factors were refined with the occupancies of all atoms fixed at those at the ideal formula (R = 0.0605). Figure 3A shows the difference Fourier map in the conduction plane at this stage. The residual electron densities at the *m*O sites were attributed to the excess K^+ ions, so that the occupancies of K^+ ion in the *BR* and *m*O sites were refined (R = 0.0398). Figure 3B shows the difference Fourier map in the

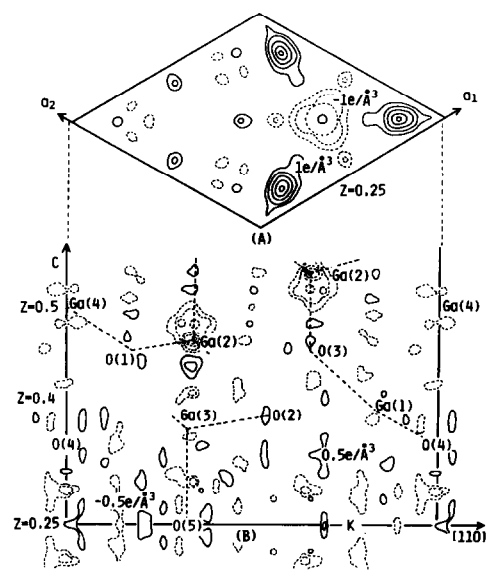

FIG. 3. Difference Fourier maps of Mg^{2+}-doped K^+-β-gallate; (A) conduction plane at Z = 0.25 when R factor is 0.0605; (B) (110) plane when R factor is 0.0398. Solid contours in (A) and (B) are drawn at intervals of 1 and $0.5e/Å^3$, respectively. Dashed contours in (A) and (B) are drawn at intervals of -1 and $-0.5e/Å^3$, respectively.

TABLE II

POSITIONAL,[a] THERMAL AND OCCUPATION PARAMETERS

	Position	Number of atoms per unit cell	X	Z	Temperature factors (Å²) × 10⁴ U_{11}	U_{22}	U_{33}	U_{13}
(A) K⁺-β-Gallate								
Ga(1)	12(k)	11.39(4)	0.83209(9)	0.10555(2)	66(2)	51(2)	61(2)	1(1)
Ga(2)	4(f)	4	$\frac{1}{3}$	0.02443(4)	43(1)	= U_{11}	45(3)	0
Ga(3)	4(f)	4	$\frac{1}{3}$	0.17481(5)	101(2)	= U_{11}	37(3)	0
Ga(4)	2(a)	2	0	0	57(2)	= U_{11}	56(5)	0
Ga(5)	12(k)	0.56(4)	0.8388(15)	0.3248(4)	33(24)	19(36)	−5(23)	−17(6)
O(1)	12(k)	12	0.1572(5)	0.0504(2)	100(10)	80(16)	43(9)	−3(6)
O(2)	12(k)	12	0.5050(6)	0.1473(2)	79(10)	79(15)	97(12)	−2(7)
O(3)	4(f)	4	$\frac{2}{3}$	0.0555(3)	76(11)	= U_{11}	57(21)	0
O(4)	4(e)	4	0	0.1429(3)	64(11)	= U_{11}	75(23)	0
O(5)	2(c)	2	$\frac{1}{3}$	$\frac{1}{4}$	1070(119)	= U_{11}	−43(31)	0
O(6)	6(h)	0.28(2)	0.8864(27)	$\frac{1}{4}$	542(87)	1030(220)	100(38)	0
K(1)	2(d)	1.45(5)	$\frac{2}{3}$	$\frac{1}{4}$	571(32)	= U_{11}	102(19)	0
K(2)	6(h)	1.19(7)	0.8864(27)	$\frac{1}{4}$	542(87)	1030(220)	100(38)	0
K(3)	2(a)	0.04(3)	0	$\frac{1}{4}$	102(312)	= U_{11}	−42(310)	0
(B) Mg^{2+}-Doped K^+-β-Gallate								
Ga(1)	12(k)	12	0.8326(2)	0.10611(3)	56(2)	48(3)	70(3)	3(2)
Ga(2)	4(f)	3.32(6)	$\frac{1}{3}$	0.02471(7)	58(4)	= U_{11}	43(6)	0
Ga(3)	4(f)	4	$\frac{1}{3}$	0.17418(7)	56(3)	= U_{11}	39(5)	0
Ga(4)	2(a)	2	0	0	58(5)	= U_{11}	72(9)	0
O(1)	12(k)	12	0.1570(8)	0.0513(2)	99(21)	25(28)	75(17)	−10(11)
O(2)	12(k)	12	0.5055(12)	0.1483(3)	50(15)	72(28)	92(22)	−18(14)
O(3)	4(f)	4	$\frac{2}{3}$	0.0566(5)	70(25)	= U_{11}	85(41)	0
O(4)	4(e)	4	0	0.1430(5)	60(20)	= U_{11}	44(40)	0
O(5)	2(c)	2	$\frac{1}{3}$	$\frac{1}{4}$	324(63)	= U_{11}	65(62)	0
K(1)	2(d)	1.37(6)	$\frac{2}{3}$	$\frac{1}{4}$	437(42)	= U_{11}	54(30)	0
K(2)	6(h)	1.64(9)	0.8813(18)	$\frac{1}{4}$	151(38)	476(107)	106(45)	0
Mg	4(f)	0.68(5)	$\frac{1}{3}$	0.02471(7)		0.035(Uiso)		
(C) NH_4^+-β-Gallate								
Ga(1)	12(k)	12	0.8323(1)	0.10584(3)	37(2)	30(3)	33(2)	1(1)
Ga(2)	4(f)	4	$\frac{1}{3}$	0.02444(7)	31(2)	= U_{11}	12(4)	0
Ga(3)	4(f)	4	$\frac{1}{3}$	0.17502(7)	45(2)	= U_{11}	12(4)	0
Ga(4)	2(a)	2	0	0	33(3)	= U_{11}	8(6)	0
O(1)	12(k)	12	0.1558(7)	0.0499(2)	75(16)	32(22)	27(14)	6(7)
O(2)	12(k)	12	0.5039(9)	0.1459(2)	66(14)	52(21)	55(17)	9(9)
O(3)	4(f)	4	$\frac{2}{3}$	0.0558(4)	34(14)	= U_{11}	23(28)	0
O(4)	4(e)	4	0	0.1412(4)	52(15)	= U_{11}	15(29)	0
O(5)	2(c)	2	$\frac{1}{3}$	$\frac{1}{4}$	704(134)	= U_{11}	−3(53)	0
N	2(d)	2	$\frac{2}{3}$	$\frac{1}{4}$	686(145)	= U_{11}	90(83)	0

[a] For all atoms $Y = 2X$, numbers in brackets correspond to estimated errors in the last digits.

(110) plane at this stage. No peaks are observed at the Ga(5) site while valleys are observed at the Ga(2) sites, which is caused by substituting Mg atoms with a smaller atomic number than Ga. Hence, in the subsequent refinements, the occupancy factors

of Mg and Ga atoms in the Ga(2) site were refined under the restriction that the total occupancy in the Ga(2) site was fixed at four atoms per unit cell (R = 0.0353). The final parameters are listed in Table II B.

(c) NH_4^+-β-Gallate

Starting positional parameters were taken from those of the final cycle of the K^+-β-gallate refinements. With the occupancy factor of the N atom, instead of NH_4^+, fixed at the ideal value, the positional parameters and anisotropic temperature factors were refined for all atoms (R = 0.0614). Difference Fourier maps calculated after the convergence are shown in Fig. 4. No significant amount of scattering is detected and all parameters at this stage are listed in Table IIC as final values.

Some interatomic distances and bond angles of each crystal are listed in Tables III and IV, respectively.

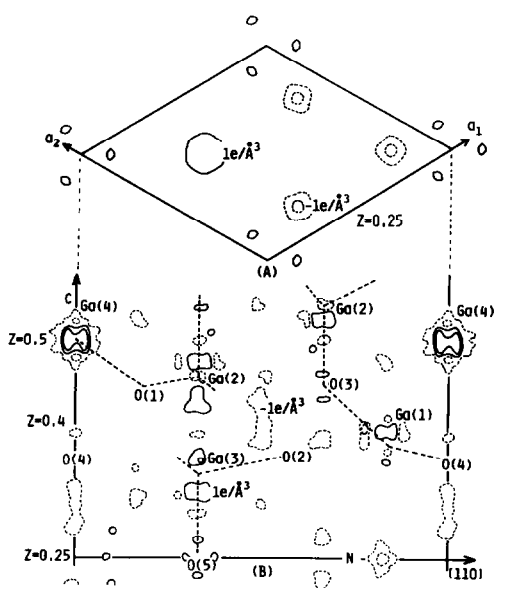

FIG. 4. Differential Fourier maps of NH_4^+-β-gallate when R factor is 0.0614; (A) conduction plane at Z = 0.25; (B) (110) plane. Solid contours are drawn at intervals of 1e/Å^3, and dashed contours at intervals of $-1e$/Å^3.

3. Charge Compensation Mechanisms

Compounds with the β-alumina type structure always contain excess alkali ions relative to the ideal composition. The Al^{3+} vacancy model was first proposed as the charge compensation mechanism for these excess positive charges (*2, 8*). Subsequently, Roth *et al.* (*20*) suggested the O^{2-} interstitial model, which indicated that Al^{3+} ions in the Al(1) sites move into an interstitial site near the conduction plane to form "Frenkel defects" and that O^{2-} ions are incorporated into the mO sites to coordinate the interstitial Al^{3+} ions. This mechanism is currently supported by many investigators (*3, 5, 15, 21*). The other mechanisms, such as incorporation of Na^+ ions into the spinel blocks (Na^+-β-gallate) (*15, 22*) or the reduction of Fe^{3+} to Fe^{2+} (β-ferrite) (*23*), have also been proposed.

West (*24*) and others (*7, 25*) have indicated the cause of the excess alkali ions over the ideal formula, $Na_2O \cdot 11Al_2O_3$. The structure of "ideal" β-alumina shows a large departure from local electroneutrality and it is improved by adding extra positive charges to the conduction plane and by removing positive charges from the spinel blocks. Wang (*26*) and Walker *et al.* (*27*) have applied simulation techniques to verify more quantitatively the discussion mentioned above.

In the present study, the refinement of the crystal structure revealed the following for K^+-β-gallate: (1) A peak of electron density is observed at the interstitial site (Ga(5), Fig. 2B); (2) The sum of the occupancies in the Ga(1) and Ga(5) sites is 11.95 atoms per unit cell (Table IIA) which agrees with the ideal value of 12; and (3) The occupancy in the Ga(5) site (0.56, Table IIA)—twice the number of the newly incorporated O^{2-} ions (O(6))—completely agrees with the amount of the excess K^+ ions determined by the chemical analysis. These results indicate that almost all Ga^{3+} ions in

TABLE III

INTERATOMIC DISTANCES

	Number of bonds	K^+-β-gallate (Å)	Mg^{2+}-doped K^+-β-gallate (Å)	NH_4^+-β-gallate (Å)
		Octahedra		
Ga(1)–O(1)	2	2.094(3)	2.086(5)	2.105(5)
–O(2)	2	1.923(3)	1.930(6)	1.910(5)
–O(3)	1	2.045(4)	2.042(7)	2.049(6)
–O(4)	1	1.910(3)	1.904(5)	1.890(4)
Ga(1)–O	(Mean)	1.998	1.966	1.995
O(1)–O(1)′	1	2.754(4)	2.759(6)	2.729(5)
–O(2)	2	2.876(5)	2.872(8)	2.869(7)
–O(3)	2	2.923(3)	2.933(5)	2.924(4)
–O(4)	2	2.689(7)	2.668(10)	2.670(10)
O(2)–O(2)′	1	2.831(4)	2.832(8)	2.851(6)
–O(3)	2	2.706(7)	2.693(12)	2.688(10)
–O(4)	2	2.921(3)	2.932(7)	2.921(5)
Ga(4)–O(1)	6	1.983(3)	1.992(6)	1.966(5)
O(1)–O(1)′	6	2.754(4)	2.759(6)	2.729(3)
O(1)″	6	2.853(5)	2.875(8)	2.831(7)
		Tetrahedra		
Ga(2)–O(1)	3	1.882(4)	1.894(6)	1.892(2)
–O(3)	1	1.876(7)	1.897(12)	1.893(10)
Ga(2)–O	(Mean)	1.881	1.895	1.892
O(1)–O(1)′	3	3.084(4)	3.099(6)	3.109(5)
–O(3)	3	3.059(7)	3.088(11)	3.072(10)
Ga(3)–O(2)	3	1.852(4)	1.848(8)	1.856(6)
–O(5)	1	1.766(1)	1.769(2)	1.769(2)
Ga(3)–O	(Mean)	1.831	1.828	1.834
O(2)–O(2)′	3	3.007(4)	3.025(8)	2.986(6)
–O(5)	3	2.971(4)	2.946(7)	3.001(6)
		Polyhedron 9-coordinated *BR*		
K(1),N–O(2)	6	2.912(3)	2.882(5)	2.957(6)
–O(5)	3	3.370(1)	2.946(5)	3.370(1)

the Ga(5) site are displaced from the Ga(1) site, and O^{2-} ions are incorporated into the *m*O sites forming Ga_i–O_i–Ga_i bridges to compensate for the positive charges of the excess K^+ ions.

In Mg^{2+}-doped K^+-β-gallate, no electron density distributions are observed at the interstitial site (Fig. 3B). Hence, it is evident that Mg^{2+}-doped gallate does not make "Frekel defects." The Ga(2)–O bond distances are lengthened by the substitution of the Mg^{2+} ion (Table III), but the occupancy of the Mg^{2+} ion at the Ga(2) site (0.68, Table 2B) is less than that determined by the chemical analysis (0.88). The discrepancy is attributed to the substitution of Mg^{2+} ions at the octahedral Ga(4) site, since the Ga–O bond distances in the $Ga(4)O_6$ octahedron are also somewhat longer than that of the undoped K^+-β-gallate (Table III). The oc-

TABLE IV

BOND ANGLES[a]

	K^+-β-gallate (deg)	Mg^{2+}-doped K^+-β-gallate (deg)	NH_4^+-β-gallate (deg)
		Octahedra	
O(1)–Ga(1)–O(1)′	82.22(11)	82.80(19)	80.83(16)
O(1)–Ga(1)–O(2)	91.33(13)	91.33(13)	91.07(20)
O(1)–Ga(1)–O(3)	89.85(14)	90.55(25)	89.49(21)
O(1)–Ga(1)–O(4)	84.26(12)	83.78(26)	83.70(23)
O(2)–Ga(1)–O(2)′	94.78(14)	94.42(25)	96.52(21)
O(2)–Ga(1)–O(3)	85.96(14)	85.33(27)	85.43(21)
O(2)–Ga(1)–O(4)	99.30(16)	99.76(26)	100.47(23)
O(1)–Ga(4)–O(1)′	87.98(12)	87.65(19)	87.89(18)
O(1)–Ga(4)–O(1)″	92.02(12)	92.35(20)	92.11(18)
		Tetrahedra	
O(1)–Ga(2)–O(1)′	110.01(13)	109.82(22)	110.45(19)
O(1)–Ga(2)–O(3)	108.93(11)	109.12(18)	108.48(16)
O(2)–Ga(3)–O(2)′	108.55(14)	109.87(29)	107.10(23)
O(2)–Ga(3)–O(5)	110.38(12)	109.07(18)	111.75(17)

[a] O–Ga–O′ expresses an angle made by two oxygens of the same layer and gallium. O–Ga–O″ expresses an angle made by two oxygens of the different layers and gallium.

cupancy of the Mg^{2+} ion at the octahedral site is related to the fact that the inverse-spinel-type structure is dominant for $MgGa_2O_4$ (*28*). In contrast, the $MgAl_2O_4$ and $CoAl_2O_4$ spinels are normal types so that divalent ions such as Mg^{2+} and Co^{2+} occupy only the tetrahedral Al(2) site in β-alumina. As a result, the following were revealed for the Mg^{2+}-doped K^+-β-gallate: (1) The positive charges of the excess K^+ ions are compensated by the substitution of Mg^{2+} ions; (2) The substitution of Mg^{2+} ions is superior to the "Frenkel defects" as a way to diminish departures from the local electroneutrality mentioned above; and (3) The difference of the amount of K^+ ions determined by the chemical analysis and calculated from the simple substitution model is attributed to the disappearance of the "Frenkel defects."

The results of the crystal structure refinements above suggest that two types of charge compensation mechanism, the "Frenkel defects" and the substitution of divalent ions, are sufficient to express the charge compensation of the positive charges. Therefore, the chemical compositions themselves speak eloquently of the charge compensation mechanisms, that is, the excess oxygen atoms in the chemical formula of K^+-β-gallate (34.28 − 34 = 0.28, Table I) are newly incorporated oxygen atoms into the *m*O site and the number of the "Frenkel defects" formed is twice as many as these oxygen atoms. For the Mg^{2+}-doped K^+-β-gallate, the amount of the excess oxygen atoms are very small so that the number of the "Frenkel defects" is negligible. Of course, these discussions have less meaning when alkali ions enter into the spinel blocks, or divalent ions incorporate into the conduction plane.

There is no virtual electron density in the difference Fourier maps of NH_4^+-β-gallate

(Fig. 4A,B). It should be emphasized the "Frenkel defects" in K^+-β-gallate disappear only by the ion exchange for NH_4^+ ions, which completely agrees with the results of the thermal analyses of the NH_4^+-β-gallate mentioned above. Though a few reports (*5, 29, 30*) have referred to the stoichiometric composition of protonic β-alumina, the disappearance of the "Frenkel defects" is clarified probably for the first time. The reason why these protonic β-alumina have stoichiometric compositions is not clear now, but it seems that the existence of protons is closely related to this phenomenon.

4. Spinel Blocks

The *c* parameters of the β-alumina type compounds decreased when divalent ions were substituted for Al^{3+} ions (6), which was also confirmed in the present study. The decrease in the *c* parameter has been considered to be caused by a tightening of the bonds connecting two spinel blocks with the increase in alkali ions (*31*) in the conduction plane. However, the results of the present study indicated that the decrease is due to the deformations of coordination polyhedra in the spinel blocks. Figure 5A indicates the movements of oxygen atoms caused by the substitution of Mg^{2+} ions in K^+-β-gallate. The thicknesses of the $Ga(1)O_6$ and $Ga(3)O_4$ polyhedra along the *c* axis decrease with the substitution of Mg^{2+} ion, which are shown by the decreases in the bonding distances of O(1)–O(4), O(2)–O(3), and O(2)–O(5) (Table III). Figure 5B indicates the movements of oxygen atoms caused by the ion exchange for NH_4^+ ions. It is notable that O(2) moves in the opposite direction to the movement of oxygen atoms in Fig. 5A. In the former, the trigger for all the movements of atoms is the expansion of the $Ga(2)O_4$ tetrahedron, which is caused by the substitution of larger Mg^{2+} ions, while in the latter the trigger is the increase of the NH_4^+–O(2) bonding distance (N–O(2)

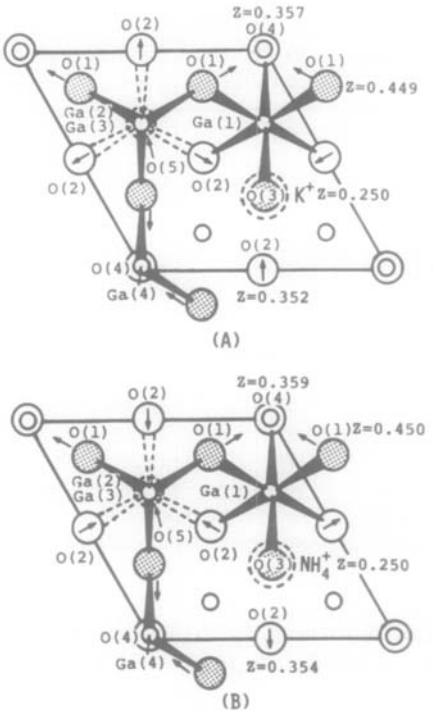

FIG. 5. Movements of oxygen atoms in spinel blocks of K^+-β-gallate projected schematically on the *ab* plane, which are caused by: (A) the substitution of Mg^{2+} ions; and (B) the ion exchange for NH_4^+ ions.

in Table III). On the other hand, the ion-exchange for NH_4^+ ions does not increase the Ga(3)–O(5) bonding distance, but increases the O(2)–Ga(3)–O(5) angle of the gallate. In contrast, the Al(3)–O(5) bonding distance of Na^+-β-alumina increased markedly with the ion exchange (*5, 32*). The cause of the discrepancy mentioned above is that the Ga(3)–O(5) bonding distance is originally longer than that of Al(3)–O(5), and it was reflected on the difference of cleavabilities between NH_4^+-β-alumina and NH_4^+-β-gallate as reported previously (*14*).

5. Conduction Plane

The number of K^+ ions at each site in the conduction plane of the K^+-β-gallate is listed in Table V. The total content of K^+ ions determined by the refinements (2.69(9)) is consistent with the result of the

TABLE V

OCCUPANCIES OF K^+ ION IN EACH SITE OF THE CONDUCTION PLANE

	BR	*mO*	*aBR*
	K^+-β-Gallate		
Obs	1.45(5)	1.19(7)	0.04(3)
Pair[a]	1.32	1.36	0
Triplet[b]	1.49	1.19	0
	Mg^{2+}-Doped K^+-β-Gallate		
Obs	1.37(6)	1.64(9)	0
Pair	0.99	2.02	0
Triplet	1.49	1.52	0

[a] Calculated from Wang's model (*30*).
[b] Calculated from Newsam's model (*31*).

chemical analysis (2.56) within the limit of error. The distributions of 2.69 K^+ ions were calculated according to Wang's pair model (*33*) and Newsam's triplet model (*34*) assuming that no K^+ ions occupied the *aBR* site, and are also listed in Table V. The distribution of K^+ ions agrees well with the triplet model as proposed by Anderson *et al.* (*15*). K^+ ions located at the *aBR* site are attributed to the thermal excitation of the *mO*–*mO* pairs to the *aBR*–*BR* pairs (*35*).

The β-alumina type compounds can contain 3.32 alkali ions per unit cell at the most (*34*). The total amount of K^+ ions (3.01(2)) of Mg^{2+}-doped K^+-β-gallate showed good agreement with that determined by the chemical analysis (2.94) and was slightly smaller than the maximum value. The K^+ ion occupancies at each site are between the two models (Table V) so that it is concluded that the conduction planes containing one, two, or three K^+ ions coexist in the Mg^{2+}-doped gallate. The probabilities of these three types of conduction plane were estimated to be 67%, 19%, and 14%, respectively.

In the case of NH_4^+-β-gallate, all NH_4^+ ions were sited only in the *BR* sites.

Conclusion

In this study, the crystal structures of K^+-β-, Mg^{2+}-doped K^+-β-, and NH_4^+-β-gallate were refined by the single crystal X-ray diffraction method and the following points were revealed:

(1) In K^+-β-gallate, the positive charges due to excess K^+ ions were compensated by O^{2-} ions in the *mO* sites which were incorporated to form the "Frenkel defects."

(2) The defect structure of K^+-β-gallate changed with the substitution of Mg^{2+} ions. That is, the excess positive charges came to be compensated by Mg^{2+} ions substituted for Ga^{3+} ions in the spinel blocks.

(3) Mg^{2+} ions entered principally into the Ga(2) sites and expanded the $Ga(2)O_4$ tetrahedron. The deformations of the coordination polyhedrons in the spinel blocks caused the decrease in the *c* parameter.

(4) The K^+ ion occupancies at each site in the conduction plane agreed well with the triplet model for K^+-β-gallate, and those of Mg^{2+}-doped K^+-β-gallate was between the triplet and the pair model.

(5) NH_4^+-β-gallate contained just a stoichiometric amount of NH_4^+ ions and no defects which permitted the existence of excess NH_4^+ ions were found.

Acknowledgments

The authors are grateful to Professor M. Kato and Dr. N. Ishizawa for use of the four-circle diffractometer. This work was supported by Special Project Research (58040052) under a Grant-in-Aid for Scientific Research of the Ministry of Education Science and Culture of Japan.

References

1. C. A. BEEVERS AND M. A. ROSS, *Z. Kristollogr.* **97,** 59 (1937).
2. C. R. PETERS, M. BETTMAN, J. W. MOORE, AND M. D. GLICK, *Acta Crystallogr. B* **27,** 1826 (1971).
3. G. COLLIN, J. P. BOILOT, A. KAHN, J. THERY,

AND R. COMES, *J. Solid State Chem.* **21,** 283 (1977).
4. W. L. ROTH, *J. Solid State Chem.* **4,** 60 (1972).
5. PH. COLOMBAN, J. P. BOILOT, A. KAHN, AND B. LUCAZEAU, *Nouv. J. Chim.* **2,** 21 (1978).
6. G. COLLIN, R. COMES, J. P. BOILOT, AND PH. COLOMBAN, *Solid State Ionics* **1,** 59 (1980).
7. T. KODAMA AND G. MUTO, *J. Solid State Chem.* **17,** 61 (1976).
8. P. D. DERNIER AND J. P. REMEIKA, *J. Solid State Chem.* **17,** 245 (1976).
9. W. A. ENGLAND, A. J. JACOBSON, AND B. C. TOFIELD, *Solid State Ionics* **6,** 21 (1982).
10. W. A. ENGLAND, A. J. JACOBSON, AND B. C. TOFIELD, *J.C.S. Chem. Commun.*, 895 (1976).
11. J. M. NEWSAM, A. K. CHEETHAM, AND B. C. TOFIELD, *Solid State Ionics* **8,** 133 (1983).
12. G. V. CHANDRASHEKHAR AND L. M. FOSTER, *J. Electrochem. Soc.* **124,** 329 (1977).
13. T. TSURUMI, H. IKAWA, K. URABE, AND S. UDAGAWA, *Yogyo-Kyokai-Shi* **91,** 553 (1983).
14. H. IKAWA, T. TSURUMI, T. NISHIMURA, K. URABE, AND S. UDAGAWA, *Solid State Ionics*, in press.
15. M. P. ANDERSON, L. M. FOSTER, AND S. J. LA PLACA, *Solid State Ionics* **5,** 211 (1981).
16. A. KAHN, J. P. BOILOT, AND J. THERY, *Mater. Res. Bull.* **11,** 397 (1976).
17. K. TANAKA, privately provided.
18. T. SAKURAI, ED., "Universal Crystallographic Computation Program System (II)," Crystallogr. Soc. Japan, 99 (1967).
19. L. M. FOSTER AND G. V. ARBACH, *J. Electrochem. Soc.* **124,** 164 (1977).
20. W. L. ROTH, F. REIDINGER, AND S. J. LA PLACE; *in* "Super Ionic Conductor" (G. D. Mahan and W. L. Roth, Eds.), p. 223, Plenum, New York (1976).
21. J. M. NEWSAM AND B. C. TOFIELD, *Solid State Ionics* **5,** 59 (1981).
22. L. M. FOSTER, *in* "Fast Ion Transport in Solids" (P. Vashishta, J. N. Mundy, and G. K. Shenoy, Eds.), p. 249, North–Holland, New York (1979).
23. J. P. BOILOT, PH. COLOMBAN, G. COLLIN, AND R. COMES, *Solid State Ionics* **1,** 69 (1980).
24. A. R. WEST, *Mater. Res. Bull.* **14,** 441 (1979).
25. H. SATO AND Y. HIROTSU, *Mater. Res. Bull.* **11,** 1307 (1976).
26. J. C. WANG, *J. Chem. Phys.* **73,** 5786 (1980).
27. J. R. WALKER AND C. R. A. CATLOW, *Nature (London)*, **286,** 473 (1980).
28. J. WEIDENBORNER, N. R. STEMPLE, AND Y. OKAYA, *Acta Crystallogr.* **20,** 761 (1966).
29. K. KATO AND H. SAALFELD, *Acta Crytstallogr. B* **33,** 1596 (1977).
30. J. D. AXE, L. M. CORLISS, J. M. HASTINGS, W. L. ROTH, AND O. HULLER, *J. Phys. Chem. Solids* **39,** 155 (1978).
31. G. J. DUDLEY AND B. C. H. STEELE, *J. Mater. Sci.* **13,** 1267 (1978).
32. S. UDAGAWA, H. IKAWA, H. TSUCHIYA, *Proc. Ann. Meeting of Ceram. Soc. Japan,* 120 (1979).
33. J. C. WANG, M. GAFFARI, AND S. CHOI, *J. Chem. Phys.* **63,** 772 (1975).
34. J. M. NEWSAM, *Solid State Ionics* **6,** 129 (1982).
35. D. WOLF, *J. Phys. Chem. Solids* **40,** 757 (1979).